City Research Online

City, University of London Institutional Repository

On the effect of realistic multicomponent diesel surrogates on cavitation and in-nozzle flow.

A. Vidal[1], P. Koukouvinis, M. Gavaises
City University of London, Department of Mechanical Engineering and Aeronautics, UK.

Abstract

Cavitation and cavitation-induced erosion highly depends on the thermodynamic properties of the fluid, which in turn affect the in-nozzle flow. However, many predictive models used today rely on constant properties or very simplified diesel surrogates. In this work, the diesel properties are predicted using a realistic four-component diesel surrogate, named J1D, which is compared with the traditionally used n-dodecane and then additised with n-hexane in amounts of 1% and 10%, named 1C6 and 10C6 respectively. The fuel property variation as function of pressure is modelled using the PC-SAFT EoS. The fluids are then used in simulations for a common rail 5-hole tip injector nozzle. The needle is assumed to be still at a lift of $105\mu m$, which is representative of the lift reached during pilot injection. The injector operating pressure is 180MPa and the collector back pressure is 5MPa. The density of the bulk fluid is assumed to vary according to a barotropic-like scheme, following an isentropic expansion. Regarding the results from the simulations, the value of mass flow rate was proportional to the liquid density of the fluids. From the results, it appears that for substances with similar viscosity and density, such as J1D, 1C6 and 10C6 the vapour pressure is dominant in the cavitation production, as the greater the vapour pressure the greater the cavitation obtained. However, when the vapour pressure is comparable, such as that for J1D and n-dodecane, the difference in density and viscosity of the fluids seems to provide the cause for a greater vaporisation the lighter the fluid is. Despite its exploratory nature, this study offers some insight into the use of complex EoS and surrogate mixtures and their effect on cavitation and preferential vaporisation in diesel.

1 INTRODUCTION

The latest studies on the demand of global energy and supply have shown that the heavy duty transportation demand may grow the most by volume (1) in the forthcoming years. As a consequence, the demand for diesel oil will rise accordingly. In addition, the current trend for modern diesel engines is to operate with upstream pressures up to 300MPa, from the nowadays 220MPa. During the discharge of the fuel through the injection holes, depressurization may lead to pressures below the liquid's saturation point, resulting in formation of cavitation; which in turn is related to injector erosion and underperformance (2). On the other hand, cavitation is also related to an enhancement in atomisation, as it increases the spray cone angle, and may provoke mass flux choke due to hampering of the free flow, enhancing then the nozzle outlet velocity (3).

A considerable amount of literature has been published on the modelling of in-nozzle cavitation. In most of the studies, the fuel is modelled as one-fluid or two-fluid mixtures, the latter combined with a mass transfer term between the phases (4). Alternatively, Eulerian-Lagrangian approximation utilising the Rayleigh-Plesset equation for modelling cavitation have been used for the tracking of dispersed bubbles and estimating the bubble growth and collapse. Other models, such as the homogeneous equilibrium model (HEM), considers the fluid as a homogeneous mixture on the sub-grid scale. This model can be used to study the formation and transport of vapour bubbles, the turbulent fluctuations in velocity and pressure and the effect of non-condensable gases (5). It has been made also possible to investigate the effect of liquid and vapour compressibility on supercavitation formation (6).

To date, in most of injector simulations the properties of the fluid in liquid state are assumed to follow a barotropic evolution, i.e. pressure and density are one to one related, if not assumed constant. On the other hand, the vapour properties are often assumed to remain constant. For the liquid, the barotropic equation has been derived in (7) following Kolev's Diesel properties collection; single component approximations using the NIST REFPROP (8) database are also available. However, the use of constant properties may lead to large deviations in the discharge coefficient and fuel heating predictions, particularly in cases of high pressure injections (9). Moreover, composition effects in Diesel fuel are related to changes in the cavitation cloud size, liquid atomisation and spray tip penetration (10). Nevertheless, the effects of using realistic surrogates and the impact of their components have not been closely examined.

Table 1: Molar composition for the diesel surrogates modelled here. Boiling points at 0.1 MPa taken from the literature.

Compound	M_w [g/mol]	T_b [K]	mol % C12	J1D	1C6	10C6
n-hexadecane	226.4	560.0	-	30.8	30.5	27.7
heptamethylnonane	226.4	520.0	-	36.5	36.3	32.9
n-dodecane	170.3	489.4	100.0	-	-	-
trans-decalin	138.2	460.5	-	6.5	6.2	5.9
1,2,4-trimethylbenzene	120.2	442.6	-	26.2	26.0	23.6
n-hexane	86.2	341.0	-	-	1.0	10.0

---

[1] Corresponding author: alvaro.vidal-roncero@city.ac.uk

The aim of the current work is to simulate the in-nozzle flow and cavitation of diesel injectors using single and multicomponent diesel surrogates, studying the differences from their outcomes, apart from assessing for the effect of very light hydrocarbons in the fuel. The surrogates are n-dodecane and a mixture of four components, named J1D and based on a grade no. 2 diesel emissions-certification fuel (11), to which n-hexane was added in a proportion of 10%, named 10C6. In their original research, J1D was tested to mimic the characteristic composition, ignition quality, volatility, density, and other properties from the real diesel fuel. The surrogate compositions are listed in Table 1.

The modelling of the surrogates is made through the PC-SAFT equation of state (EoS) (12). Several advantages are realised when using the PC-SAFT EoS compared to the widely used cubic EoS for calculating fluid properties. The PC-SAFT EoS more accurately predicts derivative properties, reducing errors by a factor of up to eight (13), as compared to predictions with a cubic EoS, such as the Peng-Robinson EoS (14). Density predictions with the PC-SAFT EoS exhibit six times lower error for a widely used surrogate such as dodecane (15). The PC-SAFT EoS provides satisfactory agreement between calculated and experimental properties of reservoir fluids, natural gas and asphaltene phase behaviour (16). These studies suggest the PC-SAFT EoS should provide reasonable predictions of diesel fuel properties at extreme operating conditions, for which a paucity of data exist.
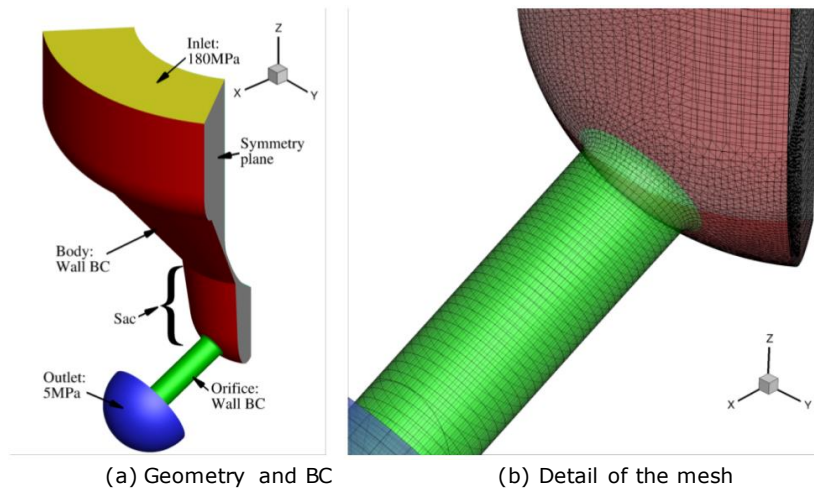

(a) Geometry and BC   (b) Detail of the mesh
Figure 1: Simulated geometry, one fifth of the total structure.

The structure of the present paper takes the form of four sections. Following the above brief introduction, the second section gives the outline of the case set-up, the CFD model used for the simulations and the description of the PC-SAFT EoS. Then, the results are shown including the calculated properties of the surrogates, in-nozzle flow, cavitation characteristics and preferential vaporisation, alongside the discussion of this results. Lastly, the final section gives a summary and critique of the findings.

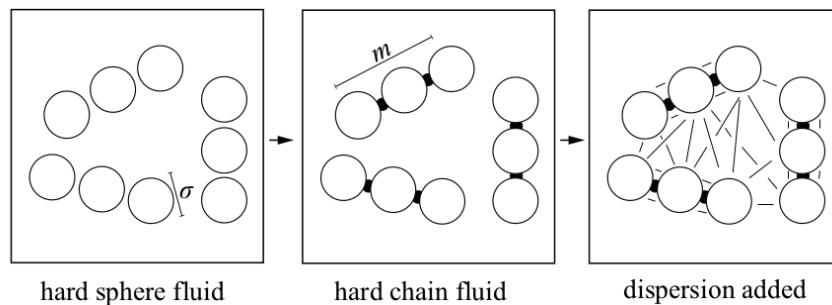hard sphere fluid   hard chain fluid   dispersion added

Figure 2: Schematic of three, non-associating molecules modelled with the PC-SAFT EoS. Each molecule is decomposed into spherical segments of diameter σ. The segments then form chains of length m that interact via dispersion forces.

2   NUMERICAL METHODS

2.1 Injector geometry and operating conditions

The examined injector geometry was based on a common rail 5-hole tip injector. As focus is given here on the effect of fuel properties, complications arising from the needle valve motion have been ignored. Although the simulation is transient, the needle was assumed to be still at a lift of $105\mu m$, similar to that reached during pilot injection. Incorporation of needle motion would obviously change the flow field, however at the expense of great computational cost and without interfering on the preferential vaporisation mechanism, which is the main topic of this work. The simulated geometry consisted on 1/5 of the full injector geometry, as shown in Figure 1a, imposing periodic boundary conditions on the symmetry planes. Moreover, constant pressure boundary conditions of 180MPa at the inlet and 5MPa at the outlet have been assumed. It must be noted that there is a hemispherical volume attached to the nozzle exit; this volume is added in order to be able to capture the complete cavitation cloud, which may extend out of the orifice.

Regarding the computational mesh, two topologies have been used, as shown in Figure 1b. Before the orifice entrance, in the sac volume, there is an unstructured tetrahedral mesh. For the rest of the domain, a hexahedral block-structured mesh is used. The total number of cells in the numerical mesh was ~200k. A finer mesh may resolve better the smaller flow scales; however, the averaged values are not expected to change significantly with regards to the cavitation process of the fuel surrogates under examination here. The Reynolds number at the needle/needle seat passage was estimated to be 7000, which corresponds to a transitional regime. Regarding the use of turbulence model, studies have shown that RANS models suffer from significant pitfalls when resolving the cavitation cloud (17), while the more accurate LES models need a significantly finer mesh, which is out of the exploratory nature of this work. However, the use of no turbulence model is related to even worse results and increased instabilities. Therefore, the turbulence model RNG $k - \omega$ SST with the Reboud correction is used.

2.2 CFD model

The in-house density-based CFD code used in this work solves the laminar, compressible and viscous Navier-Stokes system in the open-access OpenFOAM platform. The energy equation was omitted here by assuming constant entropy. Using this assumption, density is a function of pressure only, greatly simplifying the simulations. Although this is an obvious simplification, it is also an asymptotic limit that would happen for a discharge coefficient equal to unity and adiabatic walls, which can give significant insight in the in-nozzle flow. The flow has been considered compressible. Due to formation of cavitation there is a wide range of Mach numbers operating during the process, ranging from $O(10^{-1})$ to $O(10^{2})$. For density-based solvers, low Mach numbers are related to convergence problems and dispersion, so a modification in the fluxes is used for accounting for all Mach ranges. The two-phase flow is assumed to be a homogeneous mixture of vapour and liquid in mechanical equilibrium, i.e. both phases share the same pressure and velocity fields.

2.3 The PC-SAFT EoS

The PC-SAFT EoS (12) is a theoretically derived model; it splits the intermolecular potential energy of the fluid into a reference term accounting for repulsive interactions and a perturbation term accounting for attractive interactions. As shown in Figure 2, the reference fluid is composed of spherical segments comprising a hard sphere fluid that then forms molecular chains to create the hard-chain fluid. The attractive interactions, perturbations to the reference system, are accounted for with the dispersion term. Hence, each component is characterized by three pure component parameters, which are a temperature-independent segment diameter, σ, a segment interaction energy, ε, and a number of segments per molecule m. Values for the components used in this work can be found in Table 2.

Table 2: PC-SAFT pure component parameters for the compounds within the diesel surrogate mixtures listed in Table 1.

Palette Cmpd. Name	m	$\sigma(°A)$	$\epsilon/k[K]$
n-hexadecane	6.669	3.944	253.59
heptamethylnonane	5.603	4.164	266.46
n-dodecane	5.306	3.896	249.21
trans-decalin	3.291	4.067	307.98
1,2,4-trimethylbenzene	3.610	3.749	284.25
n-hexane	3.058	3.798	236.77

The PC-SAFT EoS is derived as summations of the residual Helmholtz free energy, as shown in Equation (1).

$$\frac{A^{res}}{RT} = a^{res} = a - a^{ig} = a^{hc} + a^{disp} \tag{1}$$

3

3   RESULTS AND DISCUSSION

3.1 Isentropic properties

(a) Vapour fraction

(b) Density

(c) Speed of sound

(d) Viscosity

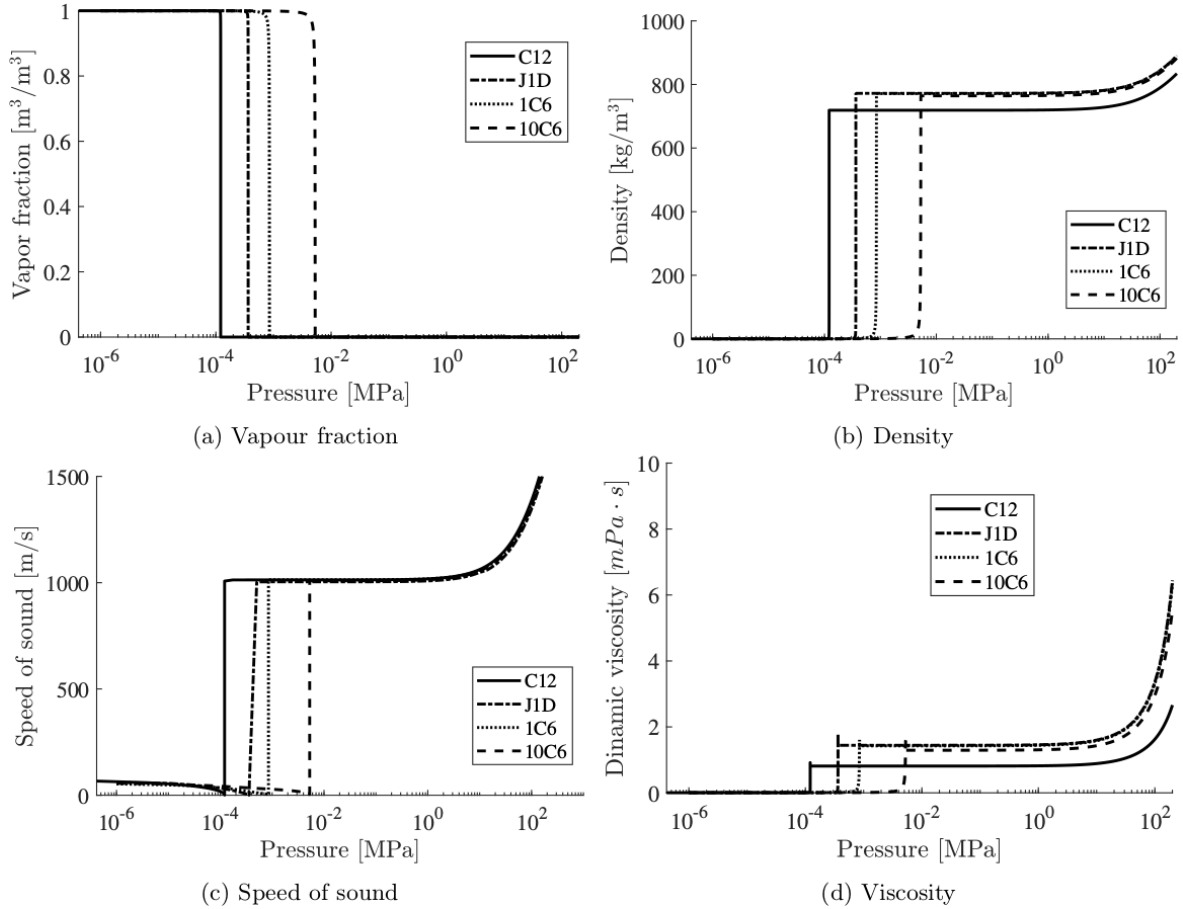**Figure 3: Isentropic lines for every surrogate. The chosen entropy is that of each substance at 324K and 5MPa, i.e. the injector outlet conditions.**

The first set of results, as shown in Figure 3, provides the isentropic properties of the surrogates studied here. The given properties as function of increasing pressure are vapour fraction, density, speed of sound and viscosity at constant entropy. As shown in Figure 3a, it is apparent that the mixture surrogate J1D has a greater vapour pressure than that of n-dodecane, and 10C6 than that the higher the content of n-hexane, the even greater vapour pressure. As a consequence, for the same depressurization value, 10C6 will be the first to vaporise, followed by 1C6, J1D and lastly n-dodecane. What is interesting about the data in this figure is that J1D is significantly heavier than n-dodecane, so one would assume that it would generally cavitate less at the same flow conditions, as most of heavier hydrocarbons would. Nevertheless, this result corroborates the findings of diesel gas chromatography (18) and it also supports the use of surrogate mixtures, as the existence of light hydrocarbons within the diesel fuel is key to its vaporisation. Figure 3b explicitly shows that n-dodecane is lighter than J1D in the liquid state. Within the mixture surrogates, J1D and 1C6 have almost identical liquid density while that of 10C6 is lower, due to the higher concentration of the lighter n-hexane.

From Figure 3c, it is clear that the speed of sound profile is similar for all surrogates within the liquid state. What is striking about the data is that as 10C6 vaporises, its speed of sound drops to $O(0.1)$m/s while the other surrogates are still liquid with speed of sounds $O(10^3)$m/s. The bump in the speed of sound seen for pressures below saturation is characteristic of the Wallis formula (19).

The greatest discrepancy is seen in viscosity, Figure 3d, where the viscosity of J1D is, at times, even three times that of n-dodecane. The spike at $p \sim p_{sat}$ is consequence of the two-phase model for viscosity (20). Similarly to what happened with density, n-dodecane viscosity is larger than that of the mixture surrogates when the latter are close to their vapour pressure.

In conclusion, J1D and 1C6 are only significantly different on the vapor pressure, with no other discernible discrepancy. On the other hand, 10C6 has also slightly lower values for density and viscosity, due to the higher concentration of n-hexane. Finally, n-dodecane differs significantly on every property apart from the speed of sound.

3.2 Hydraulic characterisation

Figures 4a and 4b show the mass flow rate and discharge coefficient for the four fluids. The value of the mass flow rate is that of the simulation when it reaches a quasi-steady state, which is one of the characteristics of the $k - \omega$ SST turbulence model. Then, if the geometry of the injector and the properties of the fluid are known, it is possible to calculate the ratio between the calculated mass flow rate and the theoretical one given by Bernoulli's equation, i.e. the discharge coefficient, using the formula:

$$C_d = \frac{\dot{m}}{A_o\sqrt{2\rho_f \Delta p}} \qquad (2)$$

where $\dot{m}$ is the calculated mass flow rate, A_o is the cross-sectional area of the orifice, ρ_f is the average density of the fluid at the end of the orifice and Δp is the difference in pressure between the inlet and the outlet of the injector. Table 3 shows the needed values for its calculation, apart from the diameter of the cylindrical orifice, which is 0.37mm, and the pressure drop along the injector, i.e. $\Delta p = p_{in} - p_{out} = 175MPa$.

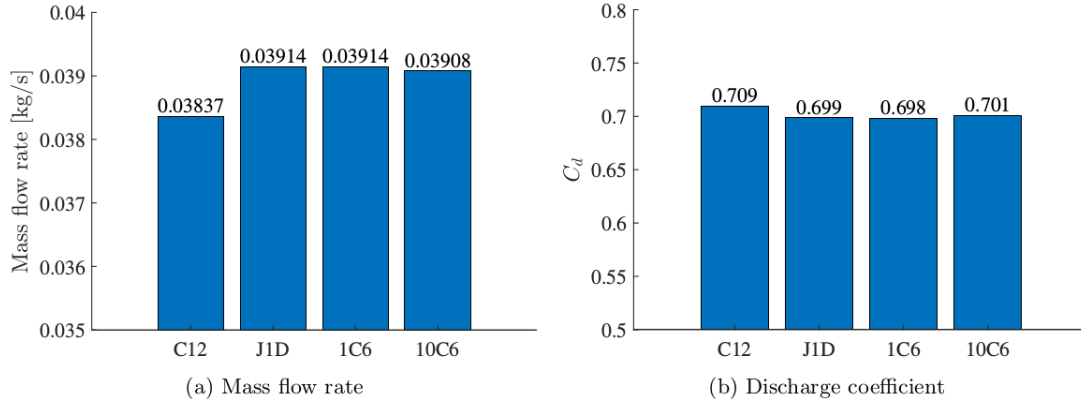(a) Mass flow rate   (b) Discharge coefficient

Figure 4: Hydraulic characterisation

Regarding the mass flow rate, overall the difference between the various fluids is not very significant. Nevertheless, it can be observed that the mass flow rate is directly related to how dense the fluid is. Thus, as $\rho J1D > \rho 1C6 > \rho 10C6 > \rho C12$, it follows that $\dot{m}J1D > \dot{m}1C6 > \dot{m}10C6 > \dot{m}C12$, which agrees with the published literature (21). The greatest difference is seen between J1D and n-dodecane, of ~2%. There is no noticeable variation between J1D and 1C6 and only a 0.02% when compared to 10C6.

Table 3: Values needed for the calculation of the discharge coefficient and the cavitation number K.

Fluid	p_{sat} [Pa]	ρ_f	K
n-dodecane	121	723	1.0286
J1D	364	776	1.0286
1C6	850	776	1.0286
10C6	5300	769	1.0285

On the other hand, the discharge coefficient shows again minimal differences between the mixtures and a rather small variation when comparing J1D with n-dodecane, of 1.4%. This result may be explained by the observation that for a cavitating nozzle, the discharge coefficient depends mainly on the cavitation number K (22), which for a certain injection, back and vapour pressure is defined as:

$$K = \frac{p_{inj} - p_v}{p_{inj} - p_{back}} \qquad (3)$$

Thus, as shown in Table 3, the cavitation number is identical between C12, J1D and 1C6, since their vapour pressures are all in the order of $O(100)$Pa and there is little difference with 10C6. Nevertheless, there exists differences between the fluids that may be accounted by how dense the fluids are or the velocities profiles during the simulations, as discussed next.

3.3 Internal flow
Figure 5 shows the velocity contours for the mid section of the injector and for all the fluids in consideration. Overall, as the kinetic energy available to accelerate the fluid $1/2\rho_f v^2$ is constant and given by the pressure difference Δp, the lighter the component the higher the velocity is expected to be. Thus, it can be observed that the greatest velocities are found in the n-dodecane case, followed by 10C6, 1C6 and finally J1D due to their increasingly higher density.
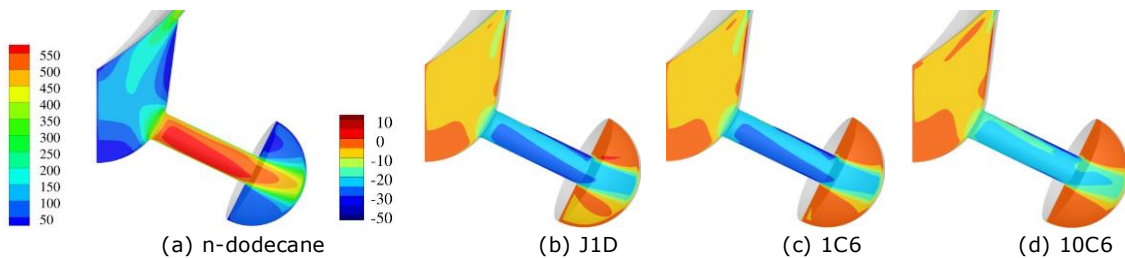

(a) n-dodecane   (b) J1D   (c) 1C6   (d) 10C6

Figure 5: Velocity contour profile for n-dodecane and the relative value for the mixture surrogates with respect to n-dodecane.

Figure 6 shows the vapour volume fraction using an isosurface of 10% orifice for n-dodecane and then it is compared with those for the mixture surrogates in Figures 6b to 6c. For that, two colors are used: blue for zones where the vapour fraction is greater for the mixtures and orange where the vapour fraction is greater for n-dodecane. As can be seen from the figure, these simulations show an unwanted creation of vapour at the exit of the orifice, due to the high velocities and change in the shape of the geometry. However, this vapour does not seem to affect the results of the simulation.

Regarding the formation of cavitation inside of the orifice, the shape and position of the vaporised volume is similar for all cases, they are located on the top surface of the orifice and it reaches its exit, decreasing the effective surface available for the free flow and therefore choking the flow. As expected, the lighter the mixture surrogate, the closer it is to the result for n-dodecane and therefore the highest differences are found against J1D. These differences are seen in two regions: the first one is found from the entrance to the orifice up to its three quarters, where the cavitation is higher for the mixture; on the other hand, at the orifice exit, the cavitation found is more intense for n-dodecane.

Once shown the volume of cavitating fluid, it is possible to calculate the amount of vapour formed through the entire length of the orifice and compare it between the different substances. Figure 7 shows the distribution of fuel vapour along the injector orifice from two perspectives. Figure 7a shows the surface covered by vapour, of any percentage different to zero, with respect to the orifice diameter, while Figure 7b shows the average of the vapour volume fraction within the non-zero values.

From the first figure, it can be clearly seen the similarity of the graphs close to the entrance and the exit of the orifice, while there is a significant disagreement along the center. This disagreement is the largest between n-dodecane and J1D, found at a relative position of 56% of the orifice, where the surface fraction covered by vapor n-dodecane is 30% larger than that for J1D. Moreover, the surface fraction given by 10C6 is very close to that of n-dodecane, while that of 1C6 is found in between but closer to J1D than to n-dodecane.

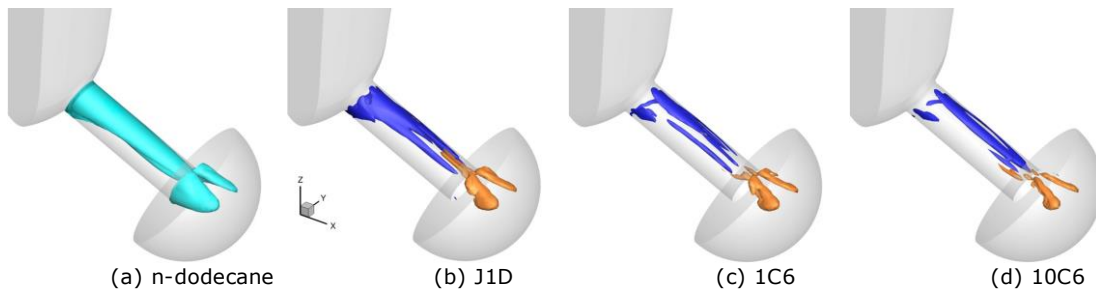(a) n-dodecane   (b) J1D   (c) 1C6   (d) 10C6

Figure 6: Vapour volume fraction isosurface at 10% for n-dodecane and the relative value for the mixture surrogates with respect to n-dodecane. The color code for the relative values is blue for higher vapour fraction and orange for a lower value than that for n-dodecane.

Surprisingly, the opposite trend is found in Figure 7b, the vapour found for J1D appears to be the most concentrated while that of n-dodecane is found to be the most diluted, although the volume of vaporised J1D is much less than that of n-dodecane. In this comparison, the biggest difference is found at a relative position of 36%, where the average vapour fraction is 26% larger than that for n-dodecane. Similarly to the previous figure, the results for 10C6 are very close to that for n-dodecane and that for 1C6 are between J1D and n-dodecane, but closer to J1D.
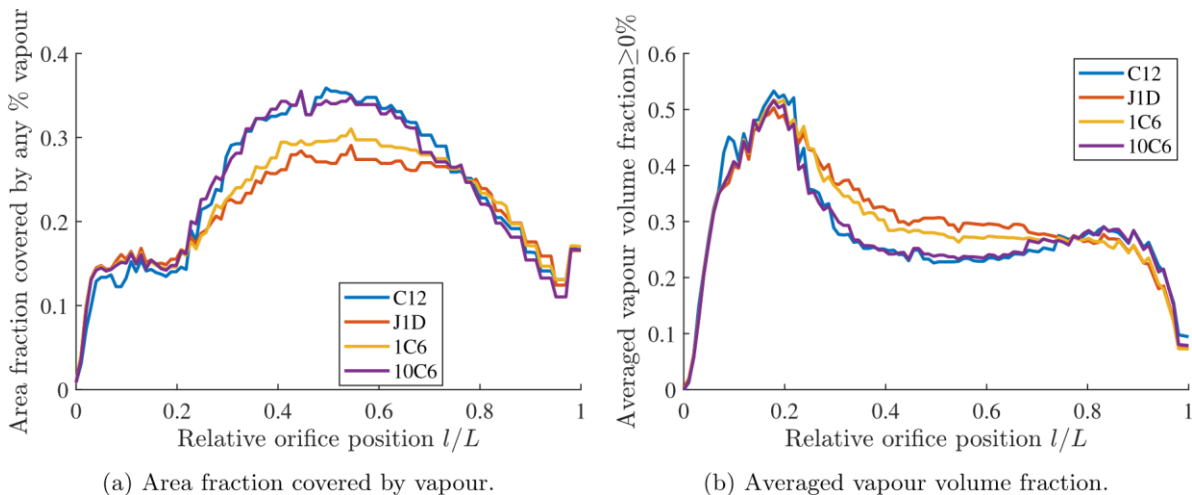

(a) Area fraction covered by vapour.   (b) Averaged vapour volume fraction.

Figure 7: Vapour distribution along the orifice.

4   SUMMARY AND CONCLUSIONS

This study has examined the impact of diesel surrogates on the in-nozzle flow and cavitation using the molecular-based PC-SAFT equation of state. For this, two surrogates have been used: n-dodecane a mixture of four components named J1D. Then, increasing additions of n-hexane where added to J1D to observe the effect of light hydrocarbons in a realistic diesel surrogate, first 1% (1C6) and then 10% (10C6). The injection process has been the same for all the cases. The geometry used was a 105μm fixed lift 5-hole injector, for which only a 1-5th was

simulated while imposing periodicity conditions at the lateral walls. The upstream/downstream pressures were fixed to 180MPa and 5MPa, respectively. The properties of the surrogates introduced in the simulations were calculated in advance by imposing a constant entropy, of that given at 324K and 5MPa, for each case.

The isentropic properties calculated show interesting results. The main differences between the n-dodecane and J1D surrogates are focused in the density and viscosity, while other properties are different only the vapour-liquid equilibrium and vapour state, with no apparent differences in the liquid phase. Although the mixture surrogates are heavier than n-dodecane, they start vaporising earlier. This result may be explained by the fact that the mixtures contain lighter hydrocarbons, influencing thus the vaporisation process by anticipating it.

Regarding the results from the simulations, the value of mass flow rate was proportional to the liquid density of the fluids. The surface fraction covered by vapor n-dodecane was 30% larger than that for J1D, however the average vapour fraction was 26% more intense for J1D than for n-dodecane. In conclusion, it appears that for substances with similar viscosity and density, such as J1D, 1C6 and 10C6 the vapour pressure is dominant in the cavitation production, as the greater the vapour pressure the greater the cavitation obtained. However, when the vapour pressure is comparable, such as that for J1D and n-dodecane, the difference in density and viscosity of the fluids seems to provide the cause for a greater vaporisation the lighter the fluid is.

Despite its exploratory nature, this study offers some insight into the use of complex EoS and surrogate mixtures and their effect on cavitation and in-nozzle flow. The findings in this report are subject to at least three limitations. Firstly, presuming an isentropic process introduces an idealism which is not able to capture such non-ideal situations as friction induced heating. Secondly, the barotropic nature of the simulations makes the mixture to be treated as a pseudo-single component, thus in every cell the global composition of the fuel is conserved. Thirdly, the turbulence model used only gives a quasi-steady state of the flow, therefore no instantaneous results can be extracted from the simulations. Further work needs to be done to establish whether more flow characteristics may be impacted using more mixture surrogates and its potential effect on spray atomisation and combustion.

5   ACKNOWLEDGEMENTS

6   REFERENCES

[1]   E. Outlook for energy: A view to 2040, 2017.

[2]   M Gavaises. Flow in valve covered orifice nozzles with cylindrical and tapered holes and link to cavitation erosion and engine exhaust emissions. *International Journal of Engine Research*, 9(6):435–447, oct 2008.

[3]   R. Payri, F.J. Salvador, J. Gimeno, and L.D. Zapata. Diesel nozzle geometry influence on spray liquid-phase fuel penetration in evaporative conditions. *Fuel*, 87(7):1165–1176, jun 2008.

[4]   Jules W. Lindau, Robert F. Kunz, David A. Boger, David R. Stinebring, and Howard J. Gibeling. High reynolds number, unsteady, multiphase CFD modeling of cavitating flows. *Journal of Fluids Engineering*, 124(3):607, 2002.

[5]   Ashok K. Singhal, Mahesh M. Athavale, Huiying Li, and Yu Jiang. Mathematical basis and validation of the full cavitation model. *Journal of Fluids Engineering*, 124(3):617, 2002.

[6]   F. Peng Karrholm, Henry Weller, and Niklas Nordin. Modelling injector flow including cavitation effects for diesel applications. In *Volume 2: Fora, Parts A and B*. ASME, 2007.

[7]   N. Kolev. *Multiphase Flow Dynamics 3: Turbulence, Gas Absorption and Release, Diesel Fuel Properties.* Springer Verlag Berlin Heidelberg, 2002.

[8]   Eric W Lemmon, Marcia L Huber, and Mark O McLinden. Nist standard reference database 23: Reference fluid thermodynamic and transport properties-refprop. 9.0. *NIST*, 2010.

[9]   George Strotos, Phoevos Koukouvinis, Andreas Theodorakakos, Manolis Gavaises, and George Bergeles. Transient heating effects in high pressure diesel injector nozzles. *International Journal of Heat and Fluid Flow*, 51:257–267, feb 2015.

[10]   Su Han Park, Se Hun Kim, and Chang Sik Lee. Mixing stability and spray behavior characteristics of diesel-ethanol-methyl ester blended fuels in a common-rail diesel injection system. *Energy & Fuels*, 23(10):5228–5235, oct 2009.

[11]   Qiaoling Wang and C. P. Chen. Simulated kinetics and chemical and physical properties of a four-component diesel surrogate fuel. *Energy & Fuels*, 31(12):13190–13197, nov 2017.

[12]   Joachim Gross and Gabriele Sadowski. Perturbed-chain SAFT: an equation of state based on a perturbation theory for chain molecules. *Industrial & Engineering Chemistry Research*, 40(4):1244–1260, feb 2001.

[13]   A.J. de Villiers, C.E. Schwarz, A.J. Burger, and G.M. Kontogeorgis. Evaluation of the PC-SAFT, SAFT and CPA equations of state in predicting derivative properties of selected non-polar and hydrogen-bonding compounds. *Fluid Phase Equilibria*, 338:1–15, jan 2013.

[14]   Ding-Yu Peng and Donald B. Robinson. A new two-constant equation of state. *Industrial & Engineering Chemistry Fundamentals*, 15(1):59–64, feb 1976.

[15]   Wei Yan, Farhad Varzandeh, and Erling H. Stenby. PVT modeling of reservoir fluids using PC-SAFT EoS and soave-BWR EoS. *Fluid Phase Equilibria*, 386:96–124, jan 2015.

[16]   Maria A. Zu´n˜iga-Hinojosa, Daimler N. Justo-Garc´ıa, Marco A. Aquino-Olivos, Luis A. Roma´nRam´ırez, and Fernando Garc´ıa-Sa´nchez. Modeling of asphaltene precipitation from n-alkane diluted heavy oils and bitumens using the PC-SAFT equation of state. *Fluid Phase Equilibria*, 376:210–224, aug 2014.

[17]   Phoevos Koukouvinis, Homa Naseri, and Manolis Gavaises. Performance of turbulence and cavitation models in prediction of incipient and developed cavitation. *International Journal of Engine Research*, 18(4):333–350, jul 2016.

[18]   Charles J. Mueller, William J. Cannella, J. Timothy Bays, Thomas J. Bruno, Kathy DeFabio, Heather D. Dettman, Rafal M. Gieleciak, Marcia L. Huber, Chol-Bum Kweon, Steven S. McConnell, William J. Pitz, and Matthew A. Ratcliff. Diesel surrogate fuels for engine testing and chemical-kinetic modeling: Compositions and properties. *Energy & Fuels*, 30(2):1445–1461, feb 2016.

[19]   Graham B. Wallis. *One-dimensional two-phase flow*. McGraw-Hill, 1969.

[20]   D. Bedeaux. The effective shear viscosity for two-phase flow. *Physica A: Statistical Mechanics and its Applications*, 121(1-2):345–361, aug 1983.

[21]   J. Dernotte, C. Hespel, F. Foucher, S. Houillˊe, and C. Mounaˤım-Rousselle. Influence of physical fuel properties on the injection rate in a diesel injector. *Fuel*, 96:153–160, jun 2012.

[22]   W. H. Nurick. Orifice cavitation and its effect on spray mixing. *Journal of Fluids Engineering*, 98(4):681, 1976.